Contents lists available at ScienceDirect

Powder Technology

Electrosprayed Poly-butyl-succinate microparticles for sustained release of Ciprofloxacin as an antimicrobial delivery system

Giorgia Puleo [a,b], Francesca Terracina [a], Valentina Catania [c], Sergio Sciré [a], Domenico Schillaci [a], Mariano Licciardi [a,*]

[a] Department of Biological, Chemical and Pharmaceutical Sciences and Technologies (STEBICEF), University of Palermo, 90123 Palermo, Italy
[b] Department of Pharmacy, University of Copenhagen, Universitetsparken 2, Copenhagen 2100, Denmark
[c] Department of Earth and Marine Sciences (DiSTeM), University of Palermo, 90128 Palermo, Italy

HIGHLIGHTS

- Electrospraying enables production of polymeric microparticles (MPs) loading drugs.
- MPs improve release of Ciprofloxacin (CPX), a poorly water-soluble antibiotic.
- Polybutylsuccinate (PBS) aids wound healing, degrades slowly, and holds promise as a biodegradable polymer.
- Electrosprayed MPs show a long release profile of CPX over long periods of time.
- MPs-PBS-CPX showed effectiveness against *S. aureus*, *P. aeruginosa* and pathogenic skin bacteria.

GRAPHICAL ABSTRACT
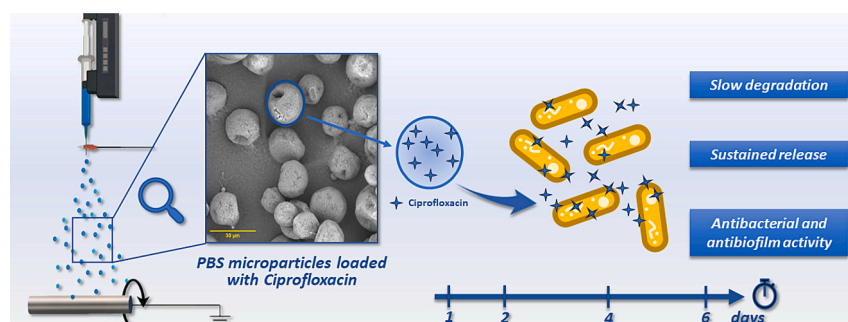
ARTICLE INFO

ABSTRACT

The increasingly complex treatment of bacterial infections, and its relevance in the clinical setting, requires the development of innovative strategies to improve patients' quality of life. In this context, polymeric microparticles represents a versatile drug delivery system (DDS) capable of improving the antibiotics' efficacy in the treatments, by loading drugs while modifying their release profile. In this study we aimed to produce polymeric microparticles by electrospraying using Poly-Butyl-Succinate (PBS), a biodegradable and biocompatible polyester. This versatile and easy-to-use technique enabled the incorporation of the poorly water-soluble Ciprofloxacin (CPX) into the polymer matrix. CPX is a fluoroquinolone antibiotic, inhibiting bacterial replication and effectively treating various infections. PBS is a well-known water-insoluble polymer with tuneable chemical-physical properties, also used for tissue regeneration and wound healing applications. An ex-vivo permeation study on porcine skin, serving as a model for human skin, was performed to assess potential enhancement in drug permeation. The microparticles were characterized by means of different techniques (SEM-EDX, XRD, ATR-FTIR, DSC), and their degradation rate was tested in DPBS and human plasma. Moreover, the as-produced DDS enabled the sustained release of CPX for several days, which proved effective against *S. aureus* and *P. aeruginosa* and also against a reference group of bacteria of skin microbiota often involved in pathological processes that make wounds chronic and difficult to heal. MIC and MBC assays were conducted using different culture media.

Effective antibacterial activity was observed, along with inhibition of *P. aeruginosa* biofilm formation at sub-MIC concentrations.

1. Introduction

Given the widespread relevance of bacterial infections on wounds to the healthcare system and patient quality of life, improving efficacy of the antibacterial treatments is crucial. [1,2] Moreover, chronic infections can play a role during tissue reparation, dysregulating the wound healing process and leading to its chronicity over time.

Clinical protocols for treating infected wounds may vary depending on the severity and type of infection. These protocols typically involve a combination of debridement, systemic antibiotics, and topical antimicrobial agents. Antiseptics are used in conjunction with antibiotics in clinical practice to treat infected wounds to reduce the presence of bacteria, accelerate the resolution of inflammation, and promote tissue healing. [3]

The use of topical antibiotics offers several advantages over systemic administration. It helps minimize systemic side effects and toxicity by delivering a high concentration of the antibacterial agent directly to the site of infection. This localized approach also reduces the likelihood of developing resistant microorganisms, as the antibiotic is primarily targeting the specific wound area. Topical antibacterial products provide flexibility in their application, allowing for both prevention and treatment of bacterial infections. [4,5]

Moreover, the development of antibiotic systems with slow release holds great promise as a strategy to address antibiotic resistance. These systems aim to avoid sub-minimum inhibitory concentration (sub-MIC) doses, which may provide selective pressure, allowing bacteria to adapt and alter their phenotype, leading to resistance. By delivering antibiotics at controlled and sustained rates, the proposed systems have the potential to maintain therapeutic levels while minimizing the risk of resistance development. [2,6]

Polymeric microparticles are excellent drug delivery systems for topical antibacterial administration. [7] They can be produced by electrospraying, which is an easy-to-use and versatile technique that can be tuned suitably to incorporate drugs in a polymer matrix. [8–10] The electrospray technique derives from electrospinning: following the application of a high electric field, when the electrostatic force applied is high enough, the solution at the tip of the needle elongates and forms a conical jet which eventually breaks into tiny droplets. As the droplets travel toward the electrically charged collector, they repel each other, remaining dispersed, the solvent evaporates, and the solid particles are collected. [11,12] This technique allows the incorporation of poorly water-soluble drugs within a polymeric matrix as microparticles. De Pieri et al. exploited electrospraying in order to delivery successfully resveratrol, which otherwise undergoes to easily degradation or depletion. The microparticles as produced were able to microencapsulate resveratrol, preserving its antioxidant properties, and tested them for the local treatment of chronic non-healing wounds. [13] Electrospraying was also employed to load several types of drugs, such as lidocaine/vancomycin/ceftazidime, into the microparticles produced by Hsu et al. [11] with analgesic and antimicrobial activity.

Ciprofloxacin (CPX) is a broad-spectrum poorly soluble fluoroquinolone antibiotic that was used as a model antibiotic in this study, despite the fact that it is not the drug of choice for topical infections, which are more often treated with mupirocin, fusidic acid, or retapamulin. [14] The rationale behind selecting CPX as the model antibiotic was its low solubility and the potential for local administration in a slow-release profile, which could act as an optimal model for DDS. By exploring the feasibility of using CPX in this context, we aim to contribute to the development of innovative therapeutic approaches.

CPX possesses several qualities that make it an attractive candidate for our research. Its broad-spectrum activity allows for effective targeting of various bacterial pathogens commonly associated with chronic wounds. Moreover, it has a well-established pharmacological profile and is widely used as a systemic antibiotic in wound healing. [15,16] Although our study does not focus on systemic antibiotics, the extensive use of CPX in wound healing supports its use as a suitable antibiotic model.

CPX stands out as optimal choice for a sustained-release polymer-based wound healing system designed to address chronic wounds, primarily due to its cost-effectiveness and remarkable antibacterial efficacy. [17,18]

Further investigation is needed to assess the applicability of this DDS to optimize the delivery of drugs specifically recommended for topical applications, such as fusidic acid and mupirocin.

For biomedical uses, such as implant devices, tissue scaffolds, and wound dressings, polymers such as poly(lactic acid) (PLA), poly-caprolactone (PCL), poly(glycolic acid) (PGA), and poly-(butylene succinate) (PBS) are in high demand. Due to their biodegradability, biocompatibility, and substantial capacity for drug loading, these polymers are perfect for these applications. [19–21] Among the several types of polymers for biomedical applications, Polybutylene-1,4-butylene succinate (PBS) offers unique advantages as it combines high biodegradability, biocompatibility, substantial drug-loading capacity, and good mechanical strength. That is also proved by the growing number of publications about its use. [22,23] PBS is a well-known water-insoluble polymer with tuneable chemical-physical properties obtained from the polycondensation reaction between succinic acid and butanediol. It is biocompatible and biodegrades at different rates depending on the application site and therefore is well suited to tissue regeneration or wound healing applications. Miceli et al. used PBS as an electrospun polymeric tubular scaffold for tissue engineering applications as a biocompatible and biodegradable material. They proved that nanofibers made of PBS provide structure and function over time and support host cell remodelling. [24] While Di Prima et al. [25] produced hydrophobic microfibrillar scaffolds employing an electrospinning technique for ocular inserts with features like wettability, mucoadhesion, and cytocompatibility. They could load triamcinolone acetonide, a lipophilic drug with a prolonged release for up to 30 days. Moreover, smooth microspheres of PBS were synthesized by Mohanray et al. for administering levodopa, a drug with poor bioavailability, short half-life, and side effects in treating Parkinson's disease. [26] Finally, Cicero et al. demonstrated that PBS scaffolds can be used as very effective agent for peripheral nerve regeneration through X-ray microcomputed tomography and magnetic resonance imaging in vivo. [27]

In the present study, we aimed to use the electrospraying technique to develop biodegradable PBS microparticles in a single solvent of chloroform (CHCl$_3$) system loaded with CPX for a sustained antimicrobial release for wound healing applications. The system thus developed showed an excellent ability to capture the drug and release it constantly for an extended period of time. Furthermore, as previously reported, the biocompatible polymer used to produce the microparticles degrades slowly, facilitating tissue regeneration and wound healing. [24,27,28] Microbiological tests showed that the microparticles exhibit antibacterial action against *S. aureus* and *P. aeruginosa*. These strains are particularly dangerous because they are considered respectively of high or critical priority categories based on their resistance as stated on the global priority list of antibiotic-resistant pathogens published by the World Health Organization (WHO). [29] In addition, tested pathogens often cause chronic infections and delay wound healing. [30] Moreover, microparticles were also tested against a reference group of bacteria of skin microbiota which can play a pathogenic role in the non-healing wound. [31]

2. Materials and methods

2.1. Materials

Poly(1,4-butylene succinate), extended with 1,6-diisocyanatohexane (PBS), Ciprofloxacin (CPX), n-octanol, Dulbecco's phosphate buffered saline (DPBS), Mueller−Hinton broth (MHB), cation-adjusted Mueller−Hinton broth (MHB2), tryptic soy agar (TSA) and crystal-violet were purchased from Sigma, Italia. Chloroform was purchased from VWR chemicals. Human plasma was extracted from volunteers upon informed consent at the University of Palermo, Palermo, Italy. For the antibacterial tests in vitro, *Staphylococcus aureus* ATCC 25923 and *Pseudomonas aeruginosa* ATCC 15442, reference strains in official tests (UNI EN European Standard), and reference skin bacteria *Staphylococcus hominis* ATCC 27844, *Staphylococcus epidermidis* ATCC 12228, *Cutibacterium acnes* ATCC 11827 and *Streptococcus agalactiae* ATCC 13813 were purchased from PBI-VWR (Italy).

2.2. Microparticles preparation by electrospraying

To prepare microparticles, CPX (5% *w/w*) was dissolved in chloroform with PBS at a concentration of 15% *w/v* by vortexing and sonicating multiple times at room temperature. Then, microparticles were obtained by electrospraying the dispersion using an electrospinning NF-103 (MECC, Japan) at room temperature and loading the dispersion into a 5 ml syringe. The flow passed through a PTFE tube connected to a 20G flat-tip needle. The electric field applied was 17.5 kV, and the feed rate was varied from 1.5 ml/h to 1.9 ml/h. The microparticles were collected on a 10 mm diameter stainless-steel rotator collector placed approximately 19 cm from the needle. The rotation speed of the collector was set at 40 rpm, and the needle moved across a transversal distance of 5 cm at a rate of 8 mm/s. Once the deposition process was complete, the microparticles were detached from the collector using a scalpel. Prior to the batch here described, several tests were conducted using various drug and polymer concentrations to enhance the incorporation efficiency and overall process yield. Additionally, the electrospraying parameters, including feed rate, applied electric field, and other variables, were also optimized. This process facilitated the replication of the batch of microparticles described above, which exhibits the processability and reproducibility compared to other batches prepared. The systems were stored under room temperature and pressure following their production.

2.3. Microparticles characterization

In order to evaluate the morphology of the as-prepared microparticles, they were observed by SEM imaging technique, using Phenom ProXSEM (Alfatest, Italy) equipped with Energy Dispersive X-ray (EDX). The SEM analysis was performed with an electron-accelerating voltage of 10 kV. Samples were prepared by dispersing the microparticles on a double-sided adhesive tape previously applied on a stainless-steel stub and dried under vacuum (0.1 Torr) before analysis. All the SEM analyses were performed at 25.0 °C ± 0.1 °C. The average diameter (d) ± standard deviation (SD) (mean ± SD, $n = 3$) of the microparticles was determined from the mean value of 100 measurements using the software ImageJ (Madison, WI, USA, version 1.46 v).

X-ray powder diffraction (XRD) patterns of MPs-PBS, pure CPX, and MPs-PBS-CPX were recorded with a Bruker D8 Advance diffractometer in the Bragg-Brentano geometry using a Ni-filtered Cu Kα radiation ($\lambda = 1.54$ Å) in the 2Θ range 5°-35° (setup conditions: tube voltage of 40 kV, current 40 mA, 0.05°/s). XRD patterns and the degree of crystallinity (DC) of each sample were analyzed and calculated using Match! 3 (Crystal Impact GbR) software.

Attenuated Total Reflectance-Fourier Transform Infrared Spectroscopy (ATR-FTIR) spectra were acquired using an FTIR Bruker Lumos model ALPHA. Spectra result from 64 scans in the wavenumber range 4000–400 cm^{-1}, with a resolution of 2 cm^{-1}. After each measurement,

the ATR diamond crystal was cleaned with a 70% ethanol/water mixture. To obtain optimum contact between the material and the ATR crystal, the microparticles were pressed against the diamond. The baseline correction has been performed by using the OPUS® software. ATR-FTIR analyzes were conducted immediately after production and again after a two-month period.

Differential scanning calorimetry (DSC) studies were carried out using a Setaram DSC131 EVO at a heating rate of 20 °C/min in the range of 20–300 °C, using 120 μl aluminum non-hermetic crucibles, with samples of 8–10 mg in the range of 20–300 °C. The analysis included the MPs with and without CPX and the drug CPX alone. DSC analyzes were conducted immediately after production and again after a two-month period.

The degradation tests were carried out in an incubator at a constant temperature of 37 °C and 5% CO_2 in two different mediums: a buffer solution of DPBS with the addition of sodium azide 0.05% *w/v* and in human plasma. The microparticles were weighted (w_0) using a precision balance, weighing about 20 mg for each sample. Then 1 ml of medium (buffer or plasma) was added to the microparticles and incubated. At precise intervals (7, 15 and 30 days), a sample was sacrificed, washed thoroughly with Milli-Q water, and filtered over a nylon filter. Then it was frozen at −80 °C and freeze-dried. The microparticles were weighed afterward. The mean recovered weight divided by the standard deviation was used to represent the findings of these three investigations, which were done in triplicate, plotting the data versus time zero.

2.4. Determination of CPX loading

To design the dissolution studies experiments, the content of CPX in PBS microparticles was first evaluated. The drug loading (DL%) was quantified using a U*V*–Vis spectrophotometer (Jasco V-760 spectrophotometer) reading at the maximum wavelength (λ max) of the CPX in chloroform of 282 nm (cuvette 1 ml, optical path 10 mm). [32,33] A standard calibration curve of CPX was formerly obtained by measuring the absorbance of known concentrations of CPX (0.1–0.001 mg/ml) in chloroform at 282 nm ($R^2 = 0.98$).

Then, a known amount of microparticles (about 10 mg) were dissolved in chloroform under magnetic stirring for about 2 h. The solution was passed through a 0.22 mm membrane filter (Millipore), and then the CPX content was evaluated by measuring the absorbance of the sample at 282 nm after suitable dilution. The drug loading (DL%) was then calculated according to the below formula:

$$DL\% = \frac{Mass\ of\ CPX\ in\ the\ microparticles}{Mass\ of\ microparticles} \times 100$$

The encapsulation efficiency (EE%) was determined by comparing the actual content of CPX with the drug content that was present in the theoretical quantity of microparticles according to the following formula:

$$EE\% = \frac{Experimentally\ calculated\ amount\ of\ CPX\ in\ the\ microparticles}{Theoretical\ amount\ of\ CPX\ in\ the\ solution} \times 100$$

2.5. In vitro dissolution studies

The in vitro release of the CPX loaded in the MPs was assessed using a metal basket that consists of a stainless steel 40 mesh construction. MPs along with an equivalent amount of pure CPX were placed into the metal basket in an empty beaker. A bi-phasic medium consisting of 100 ml of DPBS with Tween 0.05% *w/w* and 25 ml of n-octanol was then added to the beaker. [34] In this context, the in vitro model was employed to investigate the dissolution profile of drugs that exhibit poor solubility in water. [35] To ensure solubility and accurate measurement of drug release, the solubility of CPX in the release medium was carefully evaluated prior to the study.

The systems were maintained under stirring at constant temperature (150 rpm, 37 °C); these conditions were held for the entire experiment. One milliliter sample of the upper organic phase (n-octanol) was taken at regular intervals over a period of six day. The absorbance of each sample was immediately measured, allowing for the detection and quantification of CPX, and poured back into the beaker. The amount of CPX was then calculated from a standard calibration curve of CPX by measuring the absorbance of known concentrations of CPX (0.01–0.0001 mg/ml) in n-octanol at 284 nm ($R^2 = 0.99$).

It is important to note that although saturation was observed in the cumulative release of pure CPX within the experimental timeframe, an increase in the solubility of loaded CPX is still evident following the electrospray process. While this release study model may not perfectly replicate the dynamic nature of wound exudates observed in real clinical scenarios, it serves as a valuable tool to assess the constant release of drugs from the MPs within the receiving compartment and the difference between the free drug and the one incorporated into the MPs. We acknowledge the need for future studies that more closely mimic clinical conditions and validate the clinical relevance of our findings.

2.6. Ex-vivo permeation studies

Ex-vivo permeation studies were conducted using vertical Franz cells and porcine skin in an orbital shaker at 37 °C and 70 rpm as reported elsewhere. [34] The acceptor compartment contained 5 ml of n-octanol, while the donor compartment contained 0.3 ml of physiological solution with MPs-PBS-CPX or CPX alone. Samples of 200 μL were collected from the acceptor compartment at different time points (0.5, 1, 2, 4, 6, 8, and 24 h) and immediately diluted with n-octanol in order to measure the absorbance with the spectrophotometer (UV Jasco V-760) using a 1 ml cuvette with an optical path of 10 mm. Each time a sample was taken, an equal volume of n-octanol was added to the acceptor compartment to maintain sink conditions. The permeation studies were performed in triplicate, and the results were plotted as graphs of the CPX permeation over time. In addition, at the end of the permeation studies, the amount of drug remaining in the porcine skin was quantified after extraction with n-octanol from the skin used for the experiment. The amount of CPX residual in the donor compartment was quantified as well after freeze-drying of the samples and extraction of remaining CPX with n-octanol. The morphology of the skin porcine tissue was evaluated via Dino-Lite digital microscope (Dino-Lite, model AM4115T-CFVW, AnMo Electronics Corp., Hsinchu, Taiwan).

2.7. Determination of minimum inhibitory concentrations (MICs) by broth dilution micro-method

Minimum inhibitory concentrations (MICs) of the microparticles were determined toward reference strains of *S. aureus* ATCC 25923, *P. aeruginosa* ATCC 15442, *Staphylococcus hominis* ATCC 27844, *Staphylococcus epidermidis* ATCC 12228, *Cutibacterium acnes* ATCC 11827 and *Streptococcus agalactiae* ATCC 13813, by a serial dilution method by using three different media for comparative purposes, Mueller Hinton broth (MHB), Mueller Hinton Broth II (MHBII) and Tryptic Soy Broth (TSB) as previously described. [36]

Briefly, 0.1 ml of a sterile stock solution of microparticles suspended in water was added into a well of a sterile 96-well plate, and 1:2 dilution series with each broth medium was performed. The inoculum suspension was added (10 μl of a bacterial suspension from a 24 h culture containing 10^6 CFU/ml) and incubated at 37 °C for 24 h. After this time, the optical density (OD) at 570 nm was read using a spectrophotometer microplate reader (GloMax Multi Detection System TM 297 Promega, Milan, Italy). The lowest concentrations of samples whose optical density read at 570 nm was comparable with that of the negative control, which contained only inoculated broth, were considered the MICs. The accurate carrying out of the procedure is indicated by bacterial growth in the wells, marked as a positive control.

2.8. Determination of minimum bactericidal concentrations (MBCs)

In order to determine the Minimum Bactericidal concentration (MBC), we sub-cultured onto substance-free TS agar plates, 0.1 ml of each negative well, and from the positive control of MIC determinations. Then the plates were incubated at 37 °C for 24 h. The lowest concentration of the substance, which produced subcultures growing no more than three colonies, was defined as the MBC.

2.9. Biofilms susceptibility testing by using the crystal violet method

In order to determine the Minimum Bactericidal concentration (MBC), we sub-cultured onto substance-free TS agar plates, 0.1 ml of each negative well, and from the positive control of MIC determinations. Then the plates were incubated at 37 °C for 24 h. The lowest concentration of the substance, which produced subcultures growing no more than three colonies, was defined as the MBC. Sub-MIC concentrations of microparticles ranging from 1 to 0.05 μg/ml were tested for their capability of interfering with the growth as biofilm form of *P. aeruginosa* ATCC 15442, as previously reported [37]. The bacterial strain was incubated in tested tubes containing TSB with 2% *v/v* glucose at 37 °C for 24 h, then 2.5 μL of the diluted bacterial suspension (10^6 CFU/ml), was added to each well of a sterile flat-bottom 96 well loaded with 200 μL of TSB with 2% *v/v* glucose. [18] Aliquots of sub-MIC concentration of microparticles were directly added to the wells and the plates were incubated at 37 °C for 24 h. After biofilm formation, wells were washed twice with sterile NaCl 0.9% and stained with 200 μL of 0.1% *v/v* crystal violet solution for 30 min at 37 °C. The surplus solution was removed, and the plates were washed twice using tap water. After each stained well was processed, 200 μL of ethanol were added to solubilize the dye. OD was read with wavelength of 600 nm using a microplate reader (Glomax®-Multi Detection System, Promega s.r.l., Milan, Italy). The experiments were carried out at least in triplicates, and three independent experiments were performed. The percentage of biofilm inhibition formation was determined through the following formula:

$$\% \ of \ inhibition = \frac{(mean \ OD \ growth \ control - mean \ OD \ sample)}{mean \ OD \ growth \ control}$$

2.10. Statistical analysis

The mean standard deviation (SD) ($n = 3$) was used to describe the results from numerous samples. The Student's *t*-Test was used to examine statistical differences. The statistical significance level was established as *p*-value of 0.05.

3. Results and discussion

3.1. Preparation and characterization of MPs-PBS-CPX

The production of PBS nanofiber-based scaffolds obtained by electrospinning has already been discussed in previous research [25,27]. By changing the solvent used to dissolve the PBS, we observed not the formation of nanofibers but instead the formation of microparticles thus obtained by electrospraying, which can be used as drug delivery system for poor-soluble drugs. For this purpose, the experimental conditions were varied and optimized to incorporate CPX into the as-prepared microparticles. The setup of the instrument is schematized in Fig. 1a.

After production, MPs-PBS were analyzed by means of SEM in order to highlight the microscopic features and porosity structure. Fig. 1 shows representative SEM images of empty MPs (Fig. 1b) and MPs loaded with CPX (Fig. 1c). The morphologies of the microparticles were remarkably similar in both the empty and drug-loaded batches, appearing highly porous. This porosity was primarily attributed to the rapid evaporation of chloroform, facilitated by the electric field forces during the electrospraying process, leading to an enhanced surface porosity of the
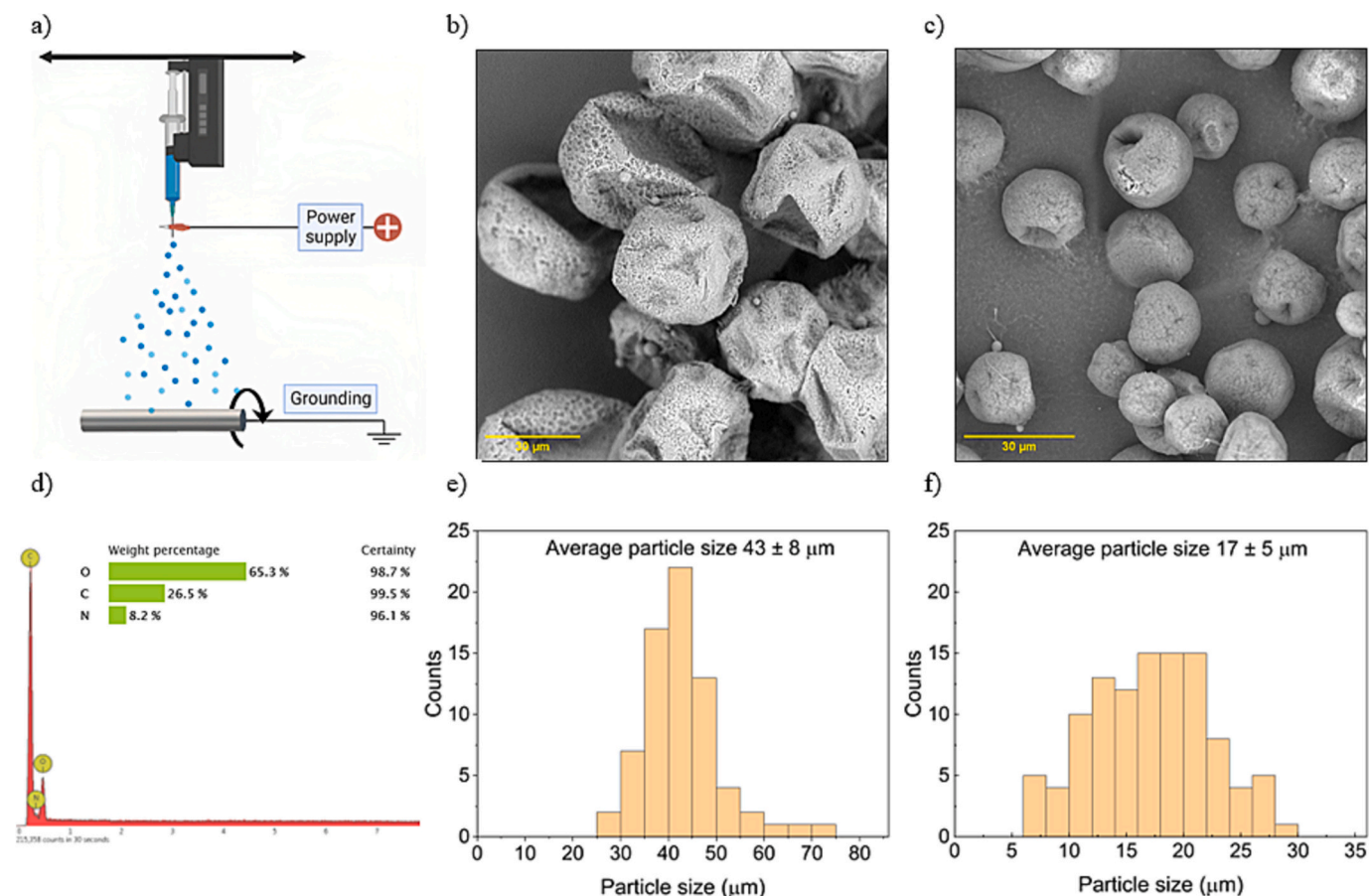
Fig. 1. a) Electrospraying setup: the arrows indicate the movements along which the needle travels during the deposition and rotation of the collector. A power supply is connected to the needle, which charges it with a positive voltage, while the collector is grounded. b) Scanning Electron Microscopy of PBS microparticles with 2050 X magnification and (c) PBS microparticles loaded with CPX with 2400 X magnification. d) EDX spectrum of microparticles of PBS made by electrospraying, after production, and relative weight percentage abundance. Size distribution of PBS microparticles (e) and PBS-CPX microparticles (f).

microparticles. [38–40]

It is possible to observe that the empty microparticles are larger than those loaded with CPX, this may suggest that the presence of CPX may influence the microparticle characteristics. It is hypothesized that factors such as surface tension and viscosity could potentially contribute to this discrepancy, as they are known to affect particle formation during electrospraying processes. [41,42] These properties can influence the behaviour of the solution during the electrospraying process, potentially leading to variations in microparticle size. In Fig. 1e and 1f, the size distributions of the microparticles are presented. The distribution of the mean diameter is centred at 43 ± 8 μm for the MPs-PBS and at 17 ± 5 μm for the MPs-PBS-CPX, indicating a more uniform size distribution for the former. These findings suggest that the presence of CPX may contribute to increased heterogeneity and smaller size of the loaded microparticles. Future studies could explore the relationship between surface tension, viscosity, and microparticle size to further elucidate the underlying mechanisms responsible for these observations.

Then, to assess if all the chloroform present in the mixture was effectively removed by evaporation during the electrospraying process, an Energy Dispersive X-ray (EDX) analysis was performed, which provides a quick non-destructive determination of the elemental composition of the sample readily identifying atoms such as chlorine, barium, potassium, and strontium, with a detection limit of about 1–10% wt. [43] In Fig. 1d it is possible to see the peaks exhibited by the microparticles, which can be attributed to carbon, oxygen, and nitrogen atoms, without any residual chlorine detection, indicating that no chloroform is retained in the final material.

The X-ray diffraction (XRD) technique was employed in this study to characterize the solid-state nature of the the target systems of our study, and in particular to assess whether the drug remained in a crystalline or amorphous state after the incorporation within the MPs. Change in the solid-state are indeed crucial to understand the properties of the drug within the MPs, including solubility, dissolution rates, and drug release kinetics.

Fig. 2a shows the XRD pattern conducted on the MPs, this analysis provides evidences supporting the presence of CPX within them. In line with previous studies [44,45] CPX showed typical crystalline peaks at $2\theta = 7.9°$, $10°$, $11.2°$, $14°$, $15.8°$, $17.7°$ and $25°$. In the sample MPs-PBS-CPX, despite the low intensity, characteristic peaks of the antibiotic are visible, which can be attributed to the limited concentration of CPX into the MPs. These distinct peaks serve as a clear indication of the presence of CPX in the loaded MPs. Furthermore, the calculation of the degree of crystallinity (DC) offers valuable insights into the structural changes induced by the presence of CPX. The degree of crystallinity represents the percentage of crystalline regions to the total material, and it is an important factor to take into account since it affects several properties. [46] A comparison of the DC values between empty MPs (59.2%) and MPs loaded with CPX (39.6%), and pure CPX (60.2%) reveals a significant alteration in the crystalline structure of the MPs loaded with CPX. The decrease in DC signifies that the incorporation of CPX results in a more amorphous nature of the MPs. The increased amorphousness observed in the CPX-loaded MPs can be attributed to the interactions between the antibiotic and the polymeric matrix of the MPs. These interactions disrupt the regular packing arrangement of the polymer chains, leading to a decrease in the long-range order and crystallinity. The presence of CPX within the MPs also hinders the growth of well-
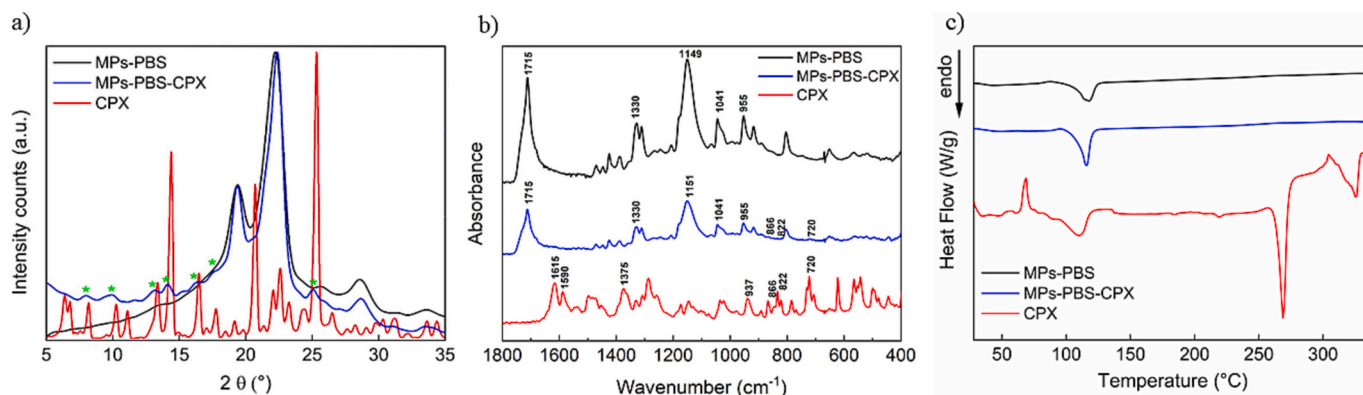
Fig. 2. a) XRD patterns of MPs-PBS (black), MPs-PBS-CPX (blue), and CPX (red). Typical peaks of CPX within the MPs-PBS-CPX sample are highlighted with a green star. b) FTIR-ATR spectra from 400 cm^{-1} to 1800 cm^{-1} of MPs-PBS (black), MPs-PBS-CPX (blue), and CPX (red). c) DSC thermograms of MPs-PBS (black), MPs-PBS-CPX (blue), and CPX (red).

defined crystal structures, further contributing to the observed decrease in crystallinity. Understanding the changes in crystallinity is of great significance as it can have a profound impact on the functional properties and behaviour of the MPs. Amorphous materials typically exhibit altered solubility, dissolution rates, and drug release kinetics compared to their crystalline counterparts.

The ATR-FTIR analysis was used to characterize the interactions between the drug and polymer as well as the absence of any degradation to the components of the formulation (Fig. 2b).

The main peak in the spectrum of CPX, identified at 1615 cm^{-1}, can be assigned to the stretching of carbonyl group C=O, while bands at 1590 and 1375 cm^{-1} are attributed to the asymmetric and symmetric vibrations of the carboxylate ion. [47,48]

These peaks were not identifiable in the MPs-PBS-CPX spectra due to the limited concentration of CPX in the MPs; nevertheless, different CPX peaks could be observed. Specifically, peaks at 707, 822, and 866 cm^{-1} [48] can be observed, which indicate the presence of CPX in the MPs-PBS-CPX sample, although with low intensity. Moreover, these peaks are not present in the unloaded microparticles' spectra. They can be attributed to the typical C—H aromatic bending, as well as δ CH (COO^{-}), which are related to the aromatic ring of CPX. [49] This data confirms the efficient incorporation of ciprofloxacin onto microparticles without any degradation.

In the PBS spectrum it is possible to observe the characteristic stretching peaks of the ester groups, in particular the stretching of the C=O and O—C—O bonds are observed at 1715 cm^{-1} and 1150 cm^{-1} respectively. [50] At 1041 cm^{-1} is possible to observe the O-C-C stretching vibration. [51] Additionally, the incorporation of CPX causes the C-O-C stretching to slightly shift toward higher wavenumbers, suggesting a non-covalent interaction between the drug and the polymer. [52]

DSC studies were performed to investigate the solid state of the as-produced systems. In Fig. 2c are shown the DSC thermograms of three samples: MPs from one component, only the polymer PBS, the MPs loaded with the drug CPX, and the drug CPX alone.

It is possible to observe that although the thermogram of the MPs-PBS-CPX is very similar to that of the MPs-sample sample, the shape of the exothermic peak is changed, in particular shifting toward lower temperatures. This change suggests that the drug, CPX, is potentially acting as a plasticizer in the polymer matrix by affecting the intermolecular forces within the polymer. This is therefore another case, as also reported by other researchers, in which the chosen therapeutic agent has a plasticizing capacity on a polymer. [26,53,54] Furthermore, the absence of the melting point peak of the CPX in the MPs-PBS-CPX thermogram can be attributed to the drug's transition to an amorphous state due to electrospraying process. This finding further corroborates the results obtained from the XRD analysis.

Moreover, both ATR-FTIR and DSC analyzes were carried out immediately after production and again after a two-month period, and were found to be the same, affirming the stability of the as-produced systems.

In Fig. 3, the residual mass of the microparticle degradation after 7, 15, and 30 days in different mediums such as DPBS and Human Plasma is shown. No significant degradation of microparticles was observed within one month. This observation suggests a potential favourable aspect of the microparticles, as their stability over time may indicate a reduced likelihood of stimulating an inflammatory response and a possibility of promoting tissue regeneration. Further studies and experimental data are needed to confirm these hypotheses.

3.2. Evaluation of dissolution and permeation properties

An in vitro dissolution study was carried out to highlight the differences in the release profiles of CPX encapsulated in the MPs compared to the pure active. In this regard, an in vitro model was used to simulate the distribution of the active molecules between the aqueous phase of the biological fluid and the lipid phase of the biological membranes. The experimental setup previously used [34] has been suitably modified to prevent the microparticles from precipitating and modifying the release. Therefore, metal baskets for the dissolution of tablets were used to evaluate how much drug was released from the microparticles into the lipidic phase.

From the results obtained in the dissolution studies (Fig. 4), it was possible to observe that tested microparticles had dissolution profiles
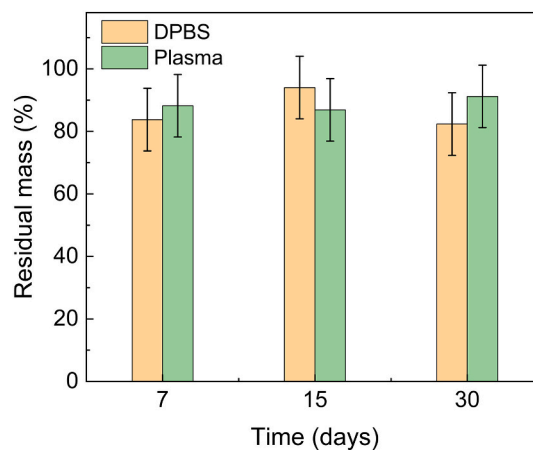

Fig. 3. Residual mass of MPs after degradation in DPBS and Plasma after 7, 15, and 30 days.
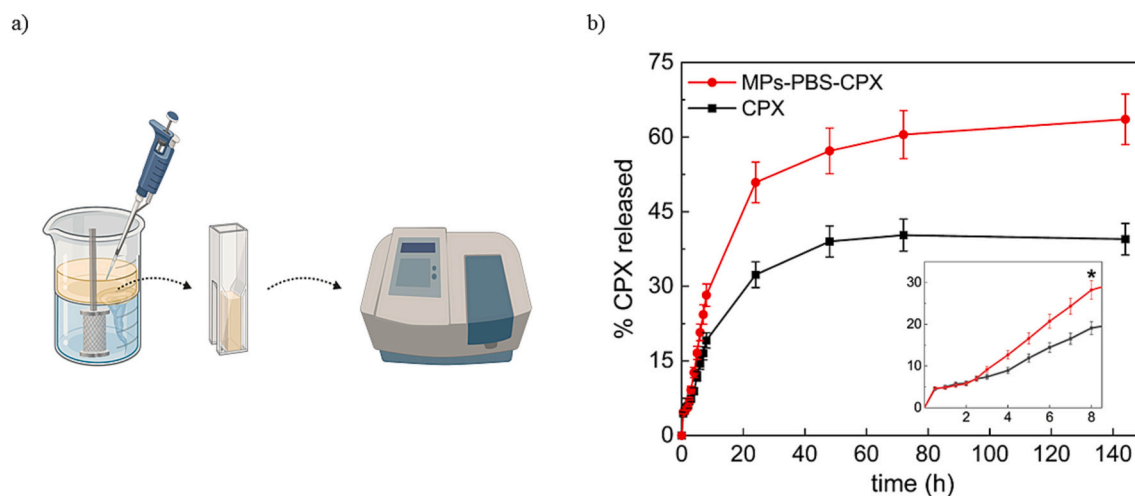
Fig. 4. a) Schematic illustration of the experimental setup: a bi-phasic system composed of buffer DPBS with Tween and n-octanol. The microparticles are loaded into the dissolution grid, and at certain time intervals, the drug concentration in the n-octanol phase is measured by a spectrophotometer. b) Graph with the percentage of CPX released as a function of time: in black pristine CPX alone, in red the CPX released from the loaded microparticles. The inset graph shows the release profile of the systems through 8 h. $p < 0.05$ (*) for the MPs versus pure CPX after 8 h.

controlled compared to the pure drug. The release of CPX is controlled and slowed thanks to their incorporation into microparticles and, at the same time, favouring the prolonged release of the drug thanks to the gradual degradation of the polymer. Incorporating CPX into the polymer matrix during the electrospraying process has indeed modified the solid-state of the drug, turning into an improvement of the solubility leading to the development of a prolonged release drug delivery system. The process by which the drug is released from the system over an extended period of time is through diffusion.

The permeation of microparticles loaded with CPX through porcine skin was investigated through an ex vivo permeation study. This experimental approach allowed to assess the potential increase in permeation of encapsulated drug through the porcine skin, which served as a model tissue for human skin.

Franz's vertical diffusion cells were employed as an in vitro ex-vivo permeation model (Fig. 5a). Despite not replicating wound conditions, using intact porcine skin as the model served two purposes. Firstly, it established a reference for normal skin permeability, enabling future comparisons with wound permeation. Secondly, it allowed for the evaluation of dermal component effects on permeation. This approach provides valuable insights before studying specific wound conditions and considers the limited availability of wound tissue samples. Overall, intact porcine skin serves as an informative starting point for evaluating permeation mechanisms and establishing a foundation for further
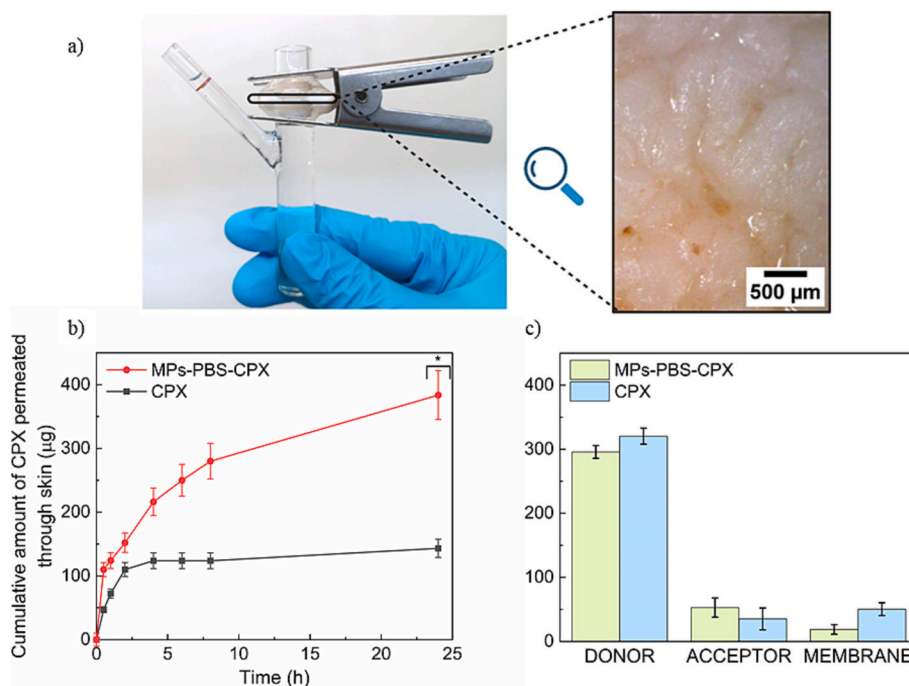

Fig. 5. a) Photo of the experimental setup for evaluating drug permeation through porcine skin using a vertical Franz cell and a close-up of the skin sample. The magnified view allows for a detailed examination of the skin's texture. b) Cumulative amount (µg) of CPX permeated through the porcine skin as a function of time until 24 h. $p < 0.05$ (*) for the tested microparticles versus pure drug after 24 h. c) Amount of residual CPX levels in different compartments: donor, acceptor, and membrane, $p < 0.05$ of microparticles versus pure drug.

studies.

Fig. 5b shows the drug release profile through the skin for 24 h. It can be stated that MPs increase drug permeation through the skin compared to the free CPX, whose permeation is slower, which can lead to accumulation and precipitation in the membrane itself, preventing effective distribution. The improved drug permeation profile through the skin in the as-produced DDS is therefore favourable, as it confirms that the electrospraying process enhances the properties of the encapsulated drug compared to the free drug, thus paving the way to other biomedical applications. Furthermore, a comparison of the residual drug levels in three different compartments: donor, acceptor, and membrane, is depicted in Fig. 5c. As a result of the improved permeation in the donor compartment, the microparticles contain a lower amount of CPX than the free drug. This, in turn, leads to a higher concentration of CPX in the acceptor compartment of the microparticles than in the one of the free CPX within the membrane while facilitating a gradual and extended transdermal crossing.

In conclusion, the encapsulation of the drug within the microparticles results in reduced retention of the drug by the membrane. This is attributed to the controlled drug release by the microparticles, which effectively prevents its accumulation and entrapment within the membrane while facilitating gradual and extended skin permeation. Additionally, the ability of the microparticles to release the drug in a gradual and prolonged manner may decrease the systemic toxicity of the drug and increase its therapeutic efficacy.

3.3. Study of antibacterial and antibiofilm activity

In addition to their potential as a drug delivery system for skin permeation applications, the microparticles studied have also been evaluated for their antibacterial properties. The minimum inhibitory concentration (MIC) and minimum bactericidal concentration (MBC) of drug-loaded microparticles have been determined against various bacterial strains, including those found on the skin. In particular, different culture media were used in antibacterial studies to evaluate the effectiveness of the drug-loaded microparticles against various bacterial strains under a range of growth conditions. The antibacterial activity in terms of MIC was found to be more effective in the Mueller Hinton-2 culture medium against the two pathogens, *S.aureus* and *P.aeruginosa* (Table 1). Furthermore, in TSB, the antibacterial activity values against the strains mentioned above are almost similar to those obtained with the MH culture medium in terms of MIC. Therefore, it is assumed that the presence of a richest medium (TSB) that promotes better microbial growth did not affect the susceptibility of the tested strains to microparticles containing ciprofloxacin than a conventional medium (MH or MHII) used in susceptibility testing. Regarding dermatological strains, no significant difference in susceptibility was observed compared to the tested medium (see Table 1).

In Table 2 are reported MBC values; a better activity for this second assay was observed, starting from the MHII medium in relation to the two pathogens, *S.aureus* and *P.aeruginosa* (Table 2). On the other hand, the MIC and MBC for the *P. aeruginosa* strain in the MH medium have the same value. In this case, the different composition of the TSB medium

Table 1
Values of MIC (μg/ml) determined in vitro by using different culture media growth (MH, MHII, TSB).

MIC (μg/mL)			
Strains	MH medium	MHII medium	TSB medium
S. aureus ATCC 25923	12.5	1.5	6.2
P. aeruginosa ATCC15442	12.5	0.75	12.5
S. hominis ATCC 27844	1.5	1.5	3.1
S. epidermidis ATCC 12228	6.2	6.2	3.1
C. acnes ATCC 11827	12.5	12.5	12.5
S. agalactiae ATCC 13813	3.1	1.5	3.1

Table 2
Values of MBC (μg/ml) determined in vitro starting from MICs obtained in different culture media growth (MH, MHII, TSB).

MBC (μg/ml)			
Strains	MH medium	MHII medium	TSB medium
S. aureus ATCC 25923	50	50	>100
P. aeruginosa ATCC15442	12.5	3.1	25
S. hominis ATCC 27844	50	>100	100
S. epidermidis ATCC 12228	50	12.5	50
C. acnes ATCC 11827	100	50	100
S. agalactiae ATCC 13813	50	25	50

has influenced the antibacterial activity in terms of MBC of the microparticles (especially for *S. aureus* and skin strains).

Furthermore, the ability of the microparticles to inhibit biofilm formation of the *P. aeruginosa* strain was tested. Sub-MIC concentrations ranging from 1 to 0.05 μg/ml were tested. The inhibition activity, expressed as a percentage of inhibition with respect to the growth control, at the screening concentration of 1 μg/ml (maximum concentration tested) is equal to 52.5%. The data was obtained from the average of three independent experiments performed individually. By comparing this result to similar studies, we found that our reported inhibition activity of 52.5% aligns with the range of values reported. [55,56] These findings further validate the potential effectiveness of MPs-PBS-CPX as a promising approach to also treat *P. aeruginosa* biofilms.

4. Conclusions

In the present study, PBS microparticles encapsulating a poorly water-soluble drug, ciprofloxacin, were successfully prepared by electrospraying to develop an effective drug delivery system for topical antibacterial therapy. Electrospraying was carried out in a single solvent system, chloroform, which evaporates and does not remain in the sample, as confirmed by elemental analysis. The system produced was fully characterized and showed good drug encapsulation properties and sustained drug release, associated with a decrease in the degree of crystallinity of CPX-loaded MPs, as confirmed by XRD analysis. The polymer used, PBS, was selected for its slow degradation, so the drug delivery system thus produced allows, on the one hand, to promote wound regeneration as it is highly biocompatible and, on the other hand, to release the drug over a long period of time, interfering with bacterial growth. In addition, results from skin permeation studies have shown that microparticles possess the ability to increase drug permeation through the skin of pigs, thus facilitating more efficient drug delivery. CPX-loaded microparticles have also been shown to counteract biofilm formation of the pathogen *P. aeruginosa*, which often colonizes chronic wounds. The drug delivery system investigated in this study holds great promise for further in vivo investigation in tissue regeneration of chronic wounds. In addition, CPX-loaded microparticles showed excellent antibacterial activity against a group of commensal skin bacteria that can engage in pathogenic behaviour in diabetic foot and venous leg ulcers and unhealed surgical wounds. [57] In addition, electrospraying has proved to be a very interesting technique that can be applied for the production of polymeric microparticles, as, by appropriately changing the parameters, different drugs can be loaded from time to time and the dosing system can be exploited for other future applications, or even multiple drugs can be combined for synergistic therapeutic action. The developed and characterized DDS is presented as a promising delivery model that can be subjected to further testing in future studies. This includes evaluating its efficacy in loading different drugs and exploring its potential applications within the field of antibacterial therapy.

CRediT authorship contribution statement

Giorgia Puleo: Formal analysis, Writing – original draft, Investigation. **Francesca Terracina:** Methodology, Writing – review & editing. **Valentina Catania:** Methodology, Data curation, Writing – review & editing. **Sergio Sciré:** Methodology, Data curation, Writing - review & editing. **Domenico Schillaci:** Investigation, Methodology, Data curation, Writing – review & editing. **Mariano Licciardi:** Conceptualization, Methodology, Writing – review & editing.

Declaration of Competing Interest

The authors declare that they have no known competing financial interests or personal relationships that could have appeared to influence the work reported in this paper.

Data availability

Data will be made available on request.

References

[1] D.I. Andersson, H. Nicoloff, K. Hjort, Mechanisms and clinical relevance of bacterial heteroresistance, Nat. Rev. Microbiol. 17 (2019) 479–496, https://doi.org/10.1038/s41579-019-0218-1.

[2] D.G.J. Larsson, C.F. Flach, Antibiotic resistance in the environment, Nat. Rev. Microbiol. 20 (2022) 257, https://doi.org/10.1038/S41579-021-00649-X.

[3] M.D. Caldwell, Bacteria and Antibiotics in Wound Healing, Surg. Clin. N. Am. 100 (2020) 757–776, https://doi.org/10.1016/j.suc.2020.05.007.

[4] L. Miranda-Calderon, C. Yus, C. Remirez de Ganuza, M. Paesa, G. Landa, E. Tapia, E. Pérez, M. Perez, V. Sebastian, S. Irusta, G. Mendoza, M. Arruebo, Combinatorial wound dressings loaded with synergistic antibiotics in the treatment of chronic infected wounds, Chem. Eng. J. 476 (2023), 146679, https://doi.org/10.1016/J.CEJ.2023.146679.

[5] Z. Li, S. Zhang, F. Zuber, S. Altenried, A. Jaklenec, R. Langer, Q. Ren, Topical application of Lactobacilli successfully eradicates *Pseudomonas aeruginosa* biofilms and promotes wound healing in chronic wounds, Microbes Infect. (2023), 105176, https://doi.org/10.1016/J.MICINF.2023.105176.

[6] P. Gao, X. Nie, M. Zou, Y. Shi, G. Cheng, Recent advances in materials for extended-release antibiotic delivery system, J. Antibiot. 64 (2011) 625–634, https://doi.org/10.1038/ja.2011.58.

[7] M.H. Xiong, Y. Bao, X.Z. Yang, Y.H. Zhu, J. Wang, Delivery of antibiotics with polymeric particles, Adv. Drug Deliv. Rev. 78 (2014), https://doi.org/10.1016/j.addr.2014.02.002.

[8] S.J. Gaskell, Electrospray: Principles and practice, J. Mass Spectrom. 32 (1997), https://doi.org/10.1002/(SICI)1096-9888(199707)32:7<677::AID-JMS536>3.0.CO;2-G.

[9] S.E. Birk, A. Boisen, L.H. Nielsen, Polymeric nano- and microparticulate drug delivery systems for treatment of biofilms, Adv. Drug Deliv. Rev. 174 (2021) 30–52, https://doi.org/10.1016/j.addr.2021.04.005.

[10] A. Tanhaei, M. Mohammadi, H. Hamishehkar, M.R. Hamblin, Electrospraying as a novel method of particle engineering for drug delivery vehicles, J. Control. Release 330 (2021) 851–865, https://doi.org/10.1016/j.jconrel.2020.10.059.

[11] Y.H. Hsu, D.W.C. Chen, M.J. Li, Y.H. Yu, Y.C. Chou, S.J. Liu, Sustained delivery of analgesic and antimicrobial agents to knee joint by direct injections of electrosprayed multipharmaceutical-loaded nano/microparticles, Polymers (Basel). 10 (2018), https://doi.org/10.3390/polym10080890.

[12] M.E. Cam, Y. Zhang, M. Edirisinghe, Electrosprayed microparticles: a novel drug delivery method, Expert Opin. Drug Deliv. 16 (2019) 895–901, https://doi.org/10.1080/17425247.2019.1648427.

[13] A. De Pieri, K. Ocorr, K. Jerreld, M. Lamoca, W. Hitzl, K. Wuertz-Kozak, Resveratrol Microencapsulation into Electrosprayed Polymeric Carriers for the Treatment of Chronic, Non-Healing Wounds, Pharmaceutics. 14 (2022), https://doi.org/10.3390/PHARMACEUTICS14040853.

[14] Y.G. Kwak, S.H. Choi, T. Kim, S.Y. Park, S.H. Seo, M.B. Kim, S.H. Choi, Clinical guidelines for the antibiotic treatment for community-acquired skin and soft tissue infection, Infect Chemother. 49 (2017) 301, https://doi.org/10.3947/IC.2017.49.4.301.

[15] S. Tripathi, B.N. Singh, D. Singh, G. Kumar, P. Srivastava, Optimization and evaluation of ciprofloxacin-loaded collagen/chitosan scaffolds for skin tissue engineering, 3 Biotech. 11 (2021) 1–17, https://doi.org/10.1007/S13205-020-02567-W/FIGURES/13.

[16] C. Cui, S. Sun, X. Li, S. Chen, S. Wu, F. Zhou, J. Ma, Optimizing the chitosan-PCL based membranes with random/aligned fiber structure for controlled ciprofloxacin delivery and wound healing, Int. J. Biol. Macromol. 205 (2022) 500–510, https://doi.org/10.1016/j.ijbiomac.2022.02.118.

[17] C. Fiorica, F.S. Palumbo, G. Pitarresi, G. Biscari, A. Martorana, C. Calà, C.M. Maida, G. Giammona, Ciprofloxacin releasing gellan gum/polydopamine based hydrogels with near infrared activated photothermal properties, Int. J. Pharm. 610 (2021), https://doi.org/10.1016/j.ijpharm.2021.121231.

[18] S. Federico, G. Pitarresi, F.S. Palumbo, C. Fiorica, V. Catania, D. Schillaci, G. Giammona, An asymmetric electrospun membrane for the controlled release of ciprofloxacin and FGF-2: evaluation of antimicrobial and chemoattractant properties, Mater. Sci. Eng. C 123 (2021), https://doi.org/10.1016/j.msec.2021.112001.

[19] P.C. Pires, F. Mascarenhas-Melo, K. Pedrosa, D. Lopes, J. Lopes, A. Macário-Soares, D. Peixoto, P.S. Giram, F. Veiga, A.C. Paiva-Santos, Polymer-based biomaterials for pharmaceutical and biomedical applications: a focus on topical drug administration, Eur. Polym. J. 187 (2023), https://doi.org/10.1016/j.eurpolymj.2023.111868.

[20] I.R. Calori, G. Braga, P. Da C.C. de Jesus, H. Bi, A.C. Tedesco, Polymer scaffolds as drug delivery systems, Eur. Polym. J. 129 (2020), https://doi.org/10.1016/j.eurpolymj.2020.109621.

[21] C.J. Cooper, A.K. Mohanty, M. Misra, Electrospinning process and structure relationship of biobased poly(butylene succinate) for nanoporous fibers, ACS Omega 3 (2018) 5547–5557, https://doi.org/10.1021/acsomega.8b00332.

[22] A. Mtibe, S. Muniyasamy, T.C. Mokhena, O. Ofosu, V. Ojijo, M. John, Recent insight into the biomedical applications of polybutylene succinate and polybutylene succinate-based materials, Express Polym Lett 17 (2023) 2–28, https://doi.org/10.3144/expresspolymlett.2023.2.

[23] M. Gigli, M. Fabbri, N. Lotti, R. Gamberini, B. Rimini, A. Munari, Poly(butylene succinate)-based polyesters for biomedical applications: a review in memory of our beloved colleague and friend Dr. Lara Finelli, Eur. Polym. J. 75 (2016) 431–460, https://doi.org/10.1016/j.eurpolymj.2016.01.016.

[24] G.C. Miceli, F.S. Palumbo, F.P. Bonomo, M. Zingales, M. Licciardi, Polybutylene succinate processing and evaluation as a micro fibrous graft for tissue engineering applications, Polymers (Basel). 14 (2022), https://doi.org/10.3390/polym14214486.

[25] G. Di Prima, M. Licciardi, F. Carfì Pavia, A.I. Lo Monte, G. Cavallaro, G. Giammona, Microfibrillar polymeric ocular inserts for triamcinolone acetonide delivery, Int. J. Pharm. 567 (2019), https://doi.org/10.1016/j.ijpharm.2019.118459.

[26] K. Mohanraj, S. Sethuraman, U.M. Krishnan, Development of poly(butylene succinate) microspheres for delivery of levodopa in the treatment of Parkinson's disease, J Biomed Mater Res B Appl Biomater 101 B (2013) 840–847, https://doi.org/10.1002/jbm.b.32888.

[27] L. Cicero, M. Licciardi, R. Cirincione, R. Puleio, G. Giammona, G. Giglia, P. Sardo, G. Edoardo Vigni, A. Cioffi, A. Sanfilippo, G. Cassata, Polybutylene succinate artificial scaffold for peripheral nerve regeneration, J Biomed Mater Res B Appl Biomater 110 (2022), https://doi.org/10.1002/jbm.b.34896.

[28] G.E. Vigni, G. Cassata, G. Caldarella, R. Cirincione, M. Licciardi, G.C. Miceli, R. Puleio, L. D'Itri, L. Lo Coco, L. Camarda, L. Cicero, Improved bone regeneration using biodegradable polybutylene succinate artificial scaffold in a rabbit model, J. Funct. Biomater. 14 (2023), https://doi.org/10.3390/jfb14010022.

[29] World Health Organization (WHO), WHO Publishes List of Bacteria for Which New Antibiotics are Urgently Needed. https://www.who.int/news/item/27-02-2017-who-publishes-list-of-bacteria-for-which-new-antibiotics-are-urgently-needed, 2017 (accessed November 2, 2023).

[30] S. DeLeon, A. Clinton, H. Fowler, J. Everett, A.R. Horswill, K.P. Rumbaugh, Synergistic interactions of *Pseudomonas aeruginosa* and *Staphylococcus aureus* in an in vitro wound model, Infect. Immun. 82 (2014) 4718–4728, https://doi.org/10.1128/IAI.02198-14.

[31] M. Tomic-Canic, J.L. Burgess, K.E. O'Neill, N. Strbo, I. Pastar, Skin microbiota and its interplay with wound healing, Am. J. Clin. Dermatol. 21 (2020) 36–43, https://doi.org/10.1007/s40257-020-00536-w.

[32] S.H. Hussein-Al-Ali, S.M. Abudoleh, Q.I.A. Abualassal, Z. Abudayeh, Y. Aldalahmah, M.Z. Hussein, Preparation and characterisation of ciprofloxacin-loaded silver nanoparticles for drug delivery, IET Nanobiotechnol. 16 (2022) 92, https://doi.org/10.1049/NBT2.12081.

[33] S. Sultana, M.S. Hossain, M. Mahmud, M. Bin Mobarak, M.H. Kabir, N. Sharmin, S. Ahmed, UV-Assisted Synthesis of Hydroxyapatite from Eggshells at Ambient Temperature: Cytotoxicity, Drug Delivery and Bioactivity, 2021, https://doi.org/10.1039/d0ra09673c.

[34] F. Terracina, R. Caruana, F.P. Bonomo, F. Montalbano, M. Licciardi, Gastro-resistant microparticles produced by spray-drying as controlled release systems for liposoluble vitamins, Pharmaceutics. 14 (2022), https://doi.org/10.3390/PHARMACEUTICS14071480.

[35] S. Azarmi, W. Roa, R. Löbenberg, Current perspectives in dissolution testing of conventional and novel dosage forms, Int. J. Pharm. 328 (2007) 12–21, https://doi.org/10.1016/J.IJPHARM.2006.10.001.

[36] M.A. Girasolo, D. Schillaci, C. Di Salvo, G. Barone, A. Silvestri, G. Ruisi, Synthesis, spectroscopic characterization and in vitro antimicrobial activity of diorganotin (IV) dichloride adducts with [1,2,4]triazolo-[1,5-a]pyrimidine and 5,7-dimethyl-[1,2,4]triazolo-[1,5-a]pyrimidine, J. Organomet. Chem. 691 (2006) 693–701, https://doi.org/10.1016/j.jorganchem.2005.10.007.

[37] A. Carbone, S. Cascioferro, B. Parrino, D. Carbone, C. Pecoraro, D. Schillaci, M. G. Cusimano, G. Cirrincione, P. Diana, Thiazole analogues of the marine alkaloid nortopsentin as inhibitors of bacterial biofilm formation, Molecules. 26 (2021), https://doi.org/10.3390/molecules26010081.

[38] D.N. Nguyen, C. Clasen, G. Van den Mooter, Pharmaceutical applications of electrospraying, J. Pharm. Sci. 105 (2016) 2601–2620, https://doi.org/10.1016/j.xphs.2016.04.024.

[39] R. Deshmukh, P. Wagh, J. Naik, Solvent evaporation and spray drying technique for micro- and nanospheres/particles preparation: a review, Dry. Technol. 34 (2016) 1758–1772, https://doi.org/10.1080/07373937.2016.1232271.

[40] S. Liu, M. Cai, R. Deng, J. Wang, R. Liang, J. Zhu, Fabrication of porous polymer microparticles with tunable pore size and density through the combination of phase separation and emulsion-solvent evaporation approach, Korea Australia Rheology Journal. 26 (2014) 63–71, https://doi.org/10.1007/s13367-014-0007-3.

[41] N. Okutan, P. Terzi, F. Altay, Affecting parameters on electrospinning process and characterization of electrospun gelatin nanofibers, Food Hydrocoll. 39 (2014) 19–26, https://doi.org/10.1016/J.FOODHYD.2013.12.022.

[42] S.H. Tan, R. Inai, M. Kotaki, S. Ramakrishna, Systematic parameter study for ultra-fine fiber fabrication via electrospinning process, Polymer (Guildf). 46 (2005) 6128–6134, https://doi.org/10.1016/J.POLYMER.2005.05.068.

[43] J.I. Goldstein, D.E. Newbury, J.R. Michael, N.W.M. Ritchie, J.H.J. Scott, D.C. Joy, Scanning Electron Microscopy and X-ray Microanalysis, 2017, https://doi.org/10.1007/978-1-4939-6676-9.

[44] H. Mesallati, A. Umerska, K.J. Paluch, L. Tajber, Amorphous polymeric drug salts as ionic solid dispersion forms of Ciprofloxacin, Mol. Pharm. 14 (2017) 2209–2223, https://doi.org/10.1021/acs.molpharmaceut.7b00039.

[45] Q. Wang, Z. Dong, Y. Du, J.F. Kennedy, Controlled release of ciprofloxacin hydrochloride from chitosan/polyethylene glycol blend films, Carbohydr. Polym. 69 (2007) 336–343, https://doi.org/10.1016/j.carbpol.2006.10.014.

[46] V. Ciaramitaro, E. Piacenza, P. Lo Meo, C. Librici, M.M. Calvino, P. Conte, G. Lazzara, D.F. Chillura Martino, From micro to macro: Physical-chemical characterization of wheat starch-based films modified with PEG200, sodium citrate, or citric acid, Int. J. Biol. Macromol. 253 (2023), https://doi.org/10.1016/j.ijbiomac.2023.127225.

[47] V.L. Dorofeev, The Betainelike Structure and Infrared Spectra of Drugs of the Fluoroquinolone Group, Pharm. Chem. J. 38 (2004) 698–702, https://doi.org/10.1007/s11094-005-0064-5.

[48] F. Tewes, J. Brillault, B. Lamy, P. Oconnell, J.C. Olivier, W. Couet, A.M. Healy, Ciprofloxacin-loaded inorganic-organic composite microparticles to treat bacterial lung infection, Mol. Pharm. 13 (2016) 100–112, https://doi.org/10.1021/acs.molpharmaceut.5b00543.

[49] M.S. Refat, W.F. El-Hawary, M.A.A. Moussa, IR, 1H NMR, mass, XRD and TGA/DTA investigations on the ciprofloxacin/iodine charge-transfer complex, Spectrochim. Acta A Mol. Biomol. Spectrosc. 78 (2011) 1356–1363, https://doi.org/10.1016/J.SAA.2011.01.010.

[50] V. Ghaffarian, S.M. Mousavi, M. Bahreini, H. Jalaei, Polyethersulfone/poly (butylene succinate) membrane: effect of preparation conditions on properties and performance, J. Ind. Eng. Chem. 20 (2014) 1359–1366, https://doi.org/10.1016/j.jiec.2013.07.019.

[51] P. Kumari Pallathadka, X.Q. Koh, A. Khatta, G.E. Luckachan, V. Mittal, Characteristics of biodegradable poly(butylene succinate) nanocomposites with thermally reduced graphene nanosheets, Polym. Compos. 38 (2017) E42–E48, https://doi.org/10.1002/pc.23824.

[52] J. Domínguez-Robles, E. Larrañeta, M.L. Fong, N.K. Martin, N.J. Irwin, P. Mutjé, Q. Tarrés, M. Delgado-Aguilar, Lignin/poly(butylene succinate) composites with antioxidant and antibacterial properties for potential biomedical applications, Int. J. Biol. Macromol. 145 (2020) 92–99, https://doi.org/10.1016/j.ijbiomac.2019.12.146.

[53] F. Siepmann, V. Le Brun, J. Siepmann, Drugs acting as plasticizers in polymeric systems: a quantitative treatment, J. Control. Release 115 (2006) 298–306, https://doi.org/10.1016/j.jconrel.2006.08.016.

[54] S. Sivasankaran, S. Jonnalagadda, Levonorgestrel loaded biodegradable microparticles for injectable contraception: Preparation, characterization and modelling of drug release, Int. J. Pharm. 624 (2022), https://doi.org/10.1016/j.ijpharm.2022.121994.

[55] P.Ø. Jensen, A. Briales, R.P. Brochmann, H. Wang, K.N. Kragh, M. Kolpen, C. Hempel, T. Bjarnsholt, N. Høiby, O. Ciofu, Formation of hydroxyl radicals contributes to the bactericidal activity of ciprofloxacin against *Pseudomonas aeruginosa*, Biofilms (2013), https://doi.org/10.1111/2049-632X.12120.

[56] A.P. Magalhães, S.P. Lopes, M.O. Pereira, Insights into cystic fibrosis polymicrobial consortia: the role of species interactions in biofilm development, phenotype, and response to in-use antibiotics, Front. Microbiol. 7 (2017) 234137, https://doi.org/10.3389/FMICB.2016.02146/BIBTEX.

[57] M.H. Swaney, L.R. Kalan, Living in your skin: microbes, molecules, and mechanisms, Infect. Immun. 89 (2021), https://doi.org/10.1128/IAI.00695-20.